Phylogeography of foot-and-mouth disease virus serotype O in Ecuador

Luiz Max Fagundes de Carvalho[1,*], Leonardo Bacelar Lima Santos[b], Nuno Rodrigues Faria[c], Waldemir de Castro Silveira[1]

[a]*Pan American Foot-and-mouth Disease Center (PANAFTOSA) – (PAHO/WHO)*
Duque de Caxias – RJ, Brazil
[b]*National Institute of Space Research – INPE*
São José dos Campos – SP , Brazil
[c]*Department of Microbiology and Immunology, Katholieke Universiteit Leuven*
Leuven, Belgium

Abstract

Foot-and-mouth disease virus (FMDV) is the causative agent of the most important disease of domestic cattle, Foot-and-Mouth Disease. In Ecuador, FMDV is maintained at an endemic state, with sporadic outbreaks. To unravel the tempo and mode of FMDV spread within the country we conducted a Bayesian phylogeographic analysis using a continuous time Markov chain (CTMC) to model the diffusion of FMDV between Ecuadorian provinces. We implement this framework through Markov Chain Monte Carlo available in the BEAST package to study 90 FMDV serotype O isolates from 17 provinces in the period 2002-2010. The Bayesian approach also allowed us to test hypotheses on the mechanisms of viral spread by incorporating environmental and epidemiological data in our prior distributions and perform Bayesian model selection. Our analyses suggest an intense flow of viral strains throughout the country that is possibly coupled to animal movements and ecological factors, since most of inferred viral spread routes were in Coast and Highland regions. Moreover, our results suggest that both short- and long-range spread occurs within Ecuador. The province of Esmeraldas, in

---

[*]Corresponding author
Email addresses: `lcarvalho@paho.org` (Luiz Max Fagundes de Carvalho),
`santoslbl@gmail.com` (Leonardo Bacelar Lima Santos),
`nuno.faria@rega.kuleuven.be` (Nuno Rodrigues Faria), `silveiraw@paho.org`
(Waldemir de Castro Silveira)

the border with Colombia and where most animal commerce is done, was found to be the most probable origin of the circulating strains, pointing to a transboundary behavior of FMDV in South America. These findings suggest that uncontrolled animal movements can create a favorable environment for FMDV maintenance and pose a serious threat to control programmes. Also, we show that phylogeographic modeling can be a powerful tool in unraveling the spatial dynamics of viruses and potentially in controlling the spread of these pathogens.

1. Introduction

Foot-and-mouth disease virus (FMDV) is a highly infectious *aphthovirus*, *Picornaviridae*, that causes the most economically important disease of domestic livestock, Foot-and-Mouth Disease (FMD). In Ecuador, the disease is maintained in endemic state and only the circulation of serotype O has been reported in recent years (Malirat et al., 2011). FMDV genomic RNA (aprox. 8200 bp) encodes 4 structural (VP1-4) proteins (Malirat et al., 2007), amongst which VP1 is a surface-exposed protein comprising 211 amino-acid residues and present in the viral capsid in 60 copies, being the most antigenic and important for vaccine design. The virus phylodynamics is marked by high rates of mutation and the same bias can be extended to VP1 (10^{-2} – 10^{-3} substitutions per site per year) (Sangula et al., 2010).

Since virus-host evolutionary interactions can be powerful at shaping viral genomes (Ploegh, 1998), viral genetic features can be used to track routes of dispersion and past demography of viral populations (Biek et al., 2007). In this sense, spatio-temporal frameworks can be useful tools to assess evolutionary patterns of pathogen spread (Araujo et al., 2009; Mondini et al., 2009), and have been previously applied to the study of FMDV dissemination (?Cottam et al., 2008; Guillot et al., 2009). Additionally, understanding FMDV evolutionary dynamics through time and space would be of interest to guide more efficient control measures and to evaluate the mechanisms of emergence of new strains.

Bayesian phylogeographic analysis (BPA) is a population modeling technique based on coalescent theory and concerns the problem of inferring the

routes of spread of an organism from molecular data. This approach is useful in tasks such as inferring most likely places of origin, migration patterns and locally-varying rates of evolution and is specially suitable to the study of viruses (Faria et al., 2011). Such tasks can be tackled by specifying a full probabilistic framework that models the process of viral spatial diffusion as a continuous time Markov Chain (CTMC) in which inference is made through Markov Chain Monte Carlo (MCMC) (Lemey et al., 2009). Importantly, this approach naturally accommodates phylogenetic uncertainty and also allows us to incorporate prior knowledge regarding important aspects about the biological processes driving viral diffusion, such as distances between locations (Lemey et al., 2009) and availability of roads and airlines (Allicock et al., 2012). BPA has been successfully applied to the study of migration patterns and epidemiological behavior of viruses (Rabaa et al., 2010; Allicock et al., 2012; Faria et al., 2012), including FMDV (Yoon et al., 2011).

This paper addresses the phylogeographic dynamics of FMDV serotype O in Ecuador by applying Bayesian phylogeographic analysis, implemented in the BEAST and SPREAD packages (Drummond and Rambaut, 2007; Bielejec et al., 2011) to 90 1D (VP1) gene sequences from FMDV isolates from 17 provinces between 2002 and 2010. Additionally, epidemiological variables such as herd size, herd density and vaccination coverage are incorporated into the analyses in order to test hypothesis on mechanisms of viral spread.

2. Material and Methods

2.1. Database Assembly

First we built a database composed by 120 FMDV serotype O 1D (VP1-encoding) gene nucleotide sequences (data obtained from NCBI, see Appendix) from eight South American countries which were aligned with MEGA 5 software using the MUSCLE algorithm (Tamura et al., 2011). This database was used to perform the Maximum Likelihood analysis (see below). From this alignment we assembled a dataset containing 90 sequences from Ecuador, representing 17 provinces in the period of 2002 to 2010.

Information on cattle herd size and density for each province was retrieved from the Ministry of Agriculture of Ecuador's website (`http://www.magap.gob.ec/mag01/`)and is provided in A.Table 2. Mean annual vaccination coverage was calculated from data on FMD vaccination in the period 2006-2010 that was obtained from the National Board for Foot-and-Mouth Disease

3

Eradication of Ecuador (CONEFA) available at `http://www.conefa.com.ec/` (see A. Table 3). To explore spatial structure in the data we calculated the global Moran I for each variable and derived approximate p-values based on 10,000 MCMC replicates.

2.2. Phylogenetic Analysis

The alignment was visually inspected and two codon deletions were detected in some of the sequences collected after 2009. The deletion at position 429 was previously reported (Maradei et al., 2011) and we were able to detect another deletion event at position 421. The dataset was corrected for this deletion by removing the gaps in the sequences, yielding a final alignment of 627 bp. We used the Recombination Analysis Tool (RAT) (Etherington et al., 2005) software to test for possible recombination events (60 nt window; 80 % similarity) and no recombination was found.

To investigate whether Ecuadorian strains shared a common geographical source we performed a Maximum Likelihood (ML) phylogenetic analysis using the whole dataset comprising 120 sequences (see Appendix, Figure 2).

In order to choose the phylogenetic model that best fitted the data we used the package jModelTest (Posada, 2008) to perform hierarchical likelihood model selection and test the fit of several models and selected the one with the lowest Bayesian Information Criterion (BIC) value. This analysis pointed the HKY+Γ model as the best fitted to our data. To further evaluate the effects of the codon deletion we conducted a separated analysis performing model selection in the complete dataset (633bp) and the gap-free dataset (627bp) and no appreciable differences were observed (data not shown).

We conducted several analyses using the BEAST package (Drummond and Rambaut, 2007) in order to find the parameter combination that provided the best fit to the data. Several molecular clock and tree priors as well as symmetric and asymmetric substitution models were tested. To perform such model selection we take advantage of recent developments in bayesian model selection (Baele et al., 2012) by estimating model marginal log-likelihood through the path sampling (PS) method and AICM (see Appendix for these results).

Based on these analyses we used the HKY85 (Hasegawa et al., 1985) phylogenetic model with gamma substitution rate heterogeneity partioned by codon position along with a relaxed exponential molecular clock (Drummond et al., 2006) and a CTMC rate prior (Ferreira and Suchard, 2008).

4

These model specifications were then applied to the dataset comprising only Ecuadorian isolates (90 sequences) in order to compute estimates and Bayesian credible interval (BCI) for the rate of molecular evolution.

2.3. Bayesian Phylogeographic Analysis

We apply the framework developed by Lemey et al, 2009 to model the spatial diffusion of FMDV between Ecuadorian provinces using a continuous time Markov chain (CTMC). This framework allows for inference on most probable routes of spread and places of origin of the circulating strains. As main strengths of the Bayesian approach we highlight its ability to accommodate phylogenetic uncertainty while providing means for formal hypothesis testing through Bayes factors (BF), i.e., by comparing the ratio of marginal likelihoods of competing models, and the incorporation of epidemiologically relevant data in the analysis. All these features are illustrated along this paper.

To investigate the effects of spatial aggregation we also performed BPA using the three ecological regions of Ecuador (Amazon, Coast and Highland) as discrete states to investigate the dynamics at a higher geographic level. Geographic signal, i.e, statistical association between phylogeny and location of origin was assessed using the software BaTS (Parker et al., 2008). Note that epidemiological data were used to perform province-level analyses only.

2.3.1. Hypothesis Testing, Model Selection and Visualization of the Results

The MCMCs were let run for 50-100 million steps and convergence was assessed by effective sample size (ESS) after a burn-in of 5-10 million steps using the Tracer 1.5 package (available at: `http://tree.bio.ed.ac.uk/software/tracer/`). In all analyses most ESS values were above 300 and all were above 100. To perform Bayesian hypothesis testing and select the best phylogeographic model we compared the marginal log-likelihood and AICM for each model. Path sampling was performed as in Baele et al (2012), using a power scheme with $\beta = 0.3$. AICM was calculated from MCMC runs using a 10% burn-in and Monte Carlo standard errors (SE) were derived using 1000 replicates (see Baele et al, 2012 for details). For all model comparisons we used equal amounts of computations, i.e., independent Monte Carlo samples.

The results from the best models were kept for the map- and tree-generation steps. The resulting maximum clade credibility (MCC) phylogenetic trees

were obtained by TreeAnnotator and generated by FigTree (`http://tree.bio.ed.ac.uk/software/figtree/`).

The results of BPA were summarized using the SPREAD (Bielejec et al., 2011) software and keyhole markup language (KML) files were generated for the inferred routes of migration and most significant rates of spread. This later analysis was carried out using Bayes factors (BF) testing. A cutoff of 6 to select most probable routes of dispersal for province-level data and a cutoff of 30 was applied to region-level data. The resulting KML files from SPREAD can be visualized in Google Earth (available at: `http://earth.google.com`) and are available as supplementary files to this article.

3. Results and Discussion

In this study we address the tempo and mode of FMDV serotype O geographical dispersal among 17 provinces of Ecuador from 2002 to 2010 using Bayesian phylogeography (Lemey et al., 2009), implemented in a full Bayesian fashion. With the advent of powerful statistical and computational techniques it became possible to conduct large-scale studies to investigate the genetic signature of pathogens, reconstruct their temporal and spatial dynamics and unravel virus-host interaction features from molecular data (Cottam et al., 2008; Biek et al., 2007; Drummond et al., 2005; Biek and Real, 2010). As virus population dynamics is inextricably coupled to that of their hosts, these rapidly evolving pathogens often carry genomic footprints of their past population dynamics (Faria et al., 2011).

3.1. Phylogenetic Analysis

We begin our study by investigating whether Ecuadorian strains shared a common event of introduction. We performed maximum likelihood (ML) analysis on a dataset containing our 90 Ecuadorian isolates and 30 sequences from South American countries covering the period 1994-2008. This analysis showed that Ecuadorian strains tend to cluster together, with some Colombian sequences interleaving Ecuadorian clusters (Appendix, A.Fig. 1). Moreover one sequence from Peru was aggregated within one Ecuadorian clade. These results point out that FMDV may have a transboundary behavior in South America, an issue that will be addressed in future studies. The strong tendency of Ecuadorian strains to cluster together, however, justifies

the study of Ecuador as independent ecotone for FMDV dynamics.

After the ML analysis we focused on the 90 Ecuadorian sequences and conducted an extensive and computationally intensive optimization study of the best parameter combination to be used in Bayesian analysis with BEAST. Several clock and demographic models were tested and model selection was done by taking advantage of path sampling (PS), a recently developed method for marginal likelihood calculation (Baele et al., 2012) and AICM, a simulation-based analogue of Akaike's information criterion (AIC) (see Appendix, A.Table 4). This analysis pointed out a skyline coalescent prior (Drummond et al., 2005) and an exponential uncorrelated clock (Drummond et al., 2006) best fitted our data, i.e., provided both higher values for marginal log-likelihood and lower values for AICM. These phylodynamic models were retained for the posterior analyses in this study and their results are discussed in more detail below.

In accordance to previous findings (Samuel and Knowles, 2001), we observed an overall picture of negative selection, as evidenced by much higher rates of substitution for the third codon position (Table 1). The high variability of FMDV can account for these findings in the sense that the virus genome evolves in error catastrophe threshold, being shaped mostly by negative selection (Balinda et al., 2010). Additionally, our Bayesian skyline plot (Fig. 5) showed a marked drop in FMDV population size over the years. This finding may be due to success of control policies such as vaccination and culling in reducing outbreak sizes (Shim and Galvani, 2009).

3.2. Phylogeographic Analysis

The maximum clade credibility trees presented in Figures 1 and 2 suggest that both temporal and spatial factors may be involved in FMDV evolution, since clades tend to be close in both space and time. The provinces with highest rates of evolution were Santo Domingo de los Tsachilas, Esmeraldas and Sucumbios (thickest branches) and the ecologic region with highest rates of evolutions was the Coast region. Using BaTS software (Parker et al., 2008), we found an association index (AI) of 0.31 (0.18-0.35 BCI) for provinces and 0.41 (0.31-0.46 BCI) for regions. These results suggest that FMDV evolution is not homogeneous throughout Ecuador but rather presents a geographic structure. This is compatible with our notion that viral evolution occurs in parallel with geographic dispersal (Faria et al., 2011).

To further explore the geographical dynamics of FMDV we conducted a

7

Bayesian phylogeographic analysis, modeling the process of viral diffusion in space through a continuous-time Markov chain (CTMC). Four aspects were studied: (i) the intensity of viral flow, i.e. the number of viral spread routes; and (ii) the association of viral dispersal with epidemiologically relevant co-variates, such as herd size and density; (iii) the geographic pattern of viral spread in both province and region levels; and (iv) the probable sources of the circulating strains.

3.2.1. Intensity scenarios

To gain insight into the number of routes of viral spread we simulate several intensity scenarios, using an intensity control parameter, ρ, to formulate the prior distribution on the number of non-zero rates in the CTMC's infinitesimal rate matrix, $\mathbf{W}$. Although any value of ρ within [0,1] would be mathematically allowed, we choose this parameter to vary within a biologically plausible range (0-0.30). These simulations allowed us to evaluate medium (ρ=0.05), high (ρ=0.10, 0.20) and very high (ρ=0.30) intensity scenarios for the viral flow in Ecuador. Each intensity scenario was evaluated against the data by comparing PS marginal likelihoods and AICM. We note that this analysis was performed taking into account differences in log-likelihood (log Bayes Factors) and AICM jointly to evaluate model ranking. The results are presented in Table 2 (see also Appendix, A.Fig. 2a) and indicate that the intensity of FMDV flow in Ecuador is compatible with scenario of medium to high intensity migration, as it was not possible to establish statistical difference between scenarios with ρ=0.05 and ρ=0.1. This pattern is expected to arise if migration routes were in average concentrated around some viral sources, like in a source-sink dispersal model (Bahl et al., 2011). The available data, though, do not allow for definitive statements to be made.

3.2.2. Incorporating epidemiological data

The second part of our phylogeographic analysis concerns the use of epidemiologically relevant data to formulate and test hypotheses on mechanisms of viral dispersal. We follow Lemey et al (2009) in their original formulation of a distance-informed prior on $\mathbf{S}$, as well as recent developments on gravity priors based on epidemiological data (Allicock et al., 2012; Bahl et al., 2011; Nelson et al., 2011). For the analyses presented here, we tested a distance-informed prior along with population (herd size) gravity, density gravity and

vaccination gravity. Details on prior specifications are given in the Appendix.

Again, models were compared by jointly considering marginal likelihoods and AICM, but now Bayes factors were calculated using a non-informative (all rates fixed to be equal) prior as a baseline. The results (Table 3) show that a population gravity model is the best explanatory variable for FMDV dispersal within Ecuador.These results are not surprising since animal movements are very likely to be connected to viral spread (Balinda et al., 2010; Cottam et al., 2008). The differences in population density and vaccination status, albeit possess some explanatory power, seem to be less important for viral spread. The similar lower performance of these two prior models is understandable since they were highly correlated (A.Fig. 2b). Specifically, the lack of detailed data for vaccination status of each province — data on vaccination was only available for 2006-2010 and we used mean annual coverage — can be a confounding factor affecting its statistical association with the data. Great-circle distance between provinces showed good explanatory power and suggests that viral spread can be proximity-driven. The better performance of the population gravity, however, suggests that long-range flow can be important as well, since differences in herd size can act as a latent variable for animal trade routes. An important limitation of these data that must be acknowledged is that the population gravity prior used here is only a surrogate for the true network of animal movements. More detailed data would undoubtedly provide basis for more accurate inference. However, taken together with the results presented above for the intensity scenarios, these findings indicate that viral flow in Ecuador tends to occur following both short- and long-range spread patterns (see below).

3.2.3. Inference on routes of spread and location of origin

To analyze the pattern of geographical spread of FMDV we used the software SPREAD (Bielejec et al., 2011) to process the trees obtained with BEAST and generate KML files that can be visualized using Google Earth. We conducted this analysis using provinces (counties) as well as ecological regions as geographic units as a way of obtaining insight into the tempo and mode of viral spread in these two levels of geographic aggregation. The results are presented in Fig. 3 and 4 and show that Ecuador has experienced intense flow of viral strains among its provinces, as evidenced by the several connections inferred. This configuration is consistent with the above intensity analysis and is very likely to occur if there is a continuous and broad

pattern of animal trade throughout the country, what seems to be true for Ecuador (Lindholm et al., 2007). The proportion of non-zero rates in the spatial transition matrix supports this high-connectivity picture, since it largely exceeds the expected for a low-diffusion model (Fig A. Figure 2a). These findings support the view that animal trade patterns represent a strong evolutive force, shaping FMDV evolution and constituting an important risk factor for FMD outbreaks (Cottam et al., 2008; Green et al., 2006).

The use of of different geographic levels allowed us to have both a detailed and an overall picture of FMDV spread throughout Ecuador. When data were aggregated to ecological regions(see A.Fig. 3), a pattern of westwards flow arose, with Coast region being the source and Highland region making connection with the Amazon region of Ecuador. Highland regions seems to play and important role as a hub since the highly significant (BF>30) rates found in BF analysis all connected this region to the other two, a result obtained using different methods as well (Carvalho et al., 2011). Moreover, this high geographic-level analysis yield a stronger phylogeographic signal, what provides evidence for long-range viral flow and also shows the importance of the level of aggregation in the search for patterns. We note however, that these results shall be considered cautiously due to the so-called ecological fallacy, that arises when drawing inference from geographical data, since different levels of aggregation can lead to drastically different conclusions (Openshaw, 1984). Nevertheless, in this study both analyses were consistent and we could notice that the province of Pichincha acted as a hub for FMDV spread together with the province of Esmeraldas. This result is not totally surprising, since these provinces have the highest incidence rates of FMD, despite having a high vaccination coverage.

In molecular epidemiology studies great interest exists on inferring the probable location of viral origin, since it can be used to guide more efficient and precise control measures through localized actions of control. The framework used in this paper naturally allows for inference on the probability of each location being the source of the circulating strains as a consequence of the probabilistic approach.

The results are reported in Table 4 and show that the most probable place of origin of Ecuadorian strains circulating in the period is the province of Esmeraldas, with an estimated coalescent time of approximately 14 years (Table 1), that points to an introduction in the end of the 1990 decade. Since this region is on the borders with Colombia, our results support the suspicion that this route may be a significant threat of spread of FMDV between

these territories (PAHO/WHO, 2008). These findings provide evidence for a transboundary pattern of flow of new strains, which is a known behavior of FMDV in other parts of the world (Balinda et al., 2010; Abdul-Hamid et al., 2011). We stress that these results should be taken with caution, since the effects of Darwinian selection and substitution saturation can bias the inferences made under the coalescent assumption. The compact nature of viral genomes calls for special statistical approaches, and efforts are already being made in this direction (Kuhnert et al., 2011).

Until 2007 the province of Esmeraldas beared the province of Santo Domingo de Los Tsachilas, where a weekly animal trade fair is carried out, bringing together farmers and animals from all over the country (Maradei et al., 2011). This may be a confounding factor for the inference of the place of origin of Ecuadorian strains, since before this year all isolates from this locality would be labeled as if coming from Esmeraldas. The results of this paper reinforce the concern that intense animal trade carried in this northern province can create a favorable environment for FMDV evolution and spread throughout the country (PAHO/WHO, 2006), posing a great threat to control programmes.

4. Conclusion

Bayesian phylogeography has proved useful in unrevealing the evolutionary dynamics of FMDV, allowing the inference on the viral routes of spread. Evidence for an intense trade pattern of infected animals among Ecuadorian provinces, as revealed by FMDV spatio-temporal genetic signature, was presented. Moreover, our phylogeographic analysis pointed the province where most of the animal trade is carried out as the source of the circulating strains along with an intense flow of viral strains in period of study.

This study also shows that the inclusion of host variables such as vaccination status, population density and routes of migration in the analysis can prove useful in unraveling other aspects of the evolutionary virus-host dynamics. A possibility that remains unexplored in this study is to explicitly test a source-sink model for FMDV dispersal within Ecuador. This approach could prove useful in an epidemiological context, as we would be able to more precisely infer viral sources and thus provide basis for more precise epidemiologic intervention, although we note that good results would depend on more detailed data, that are unavailable for Ecuador at the time.

5. Acknowledgments

References

Abdul-Hamid, N. F., Hussein, N. M., Wadsworth, J., Radford, A. D., Knowles, N. J., King, D. P., 2011. Phylogeography of foot-and-mouth disease virus types O and A in Malaysia and surrounding countries. Infect. Genet. Evol. 11, 320–328.

Allicock, O. M., Lemey, P., Tatem, A. J., Pybus, O. G., Bennett, S. N., Mueller, B. A., Suchard, M. A., Foster, J. E., Rambaut, A., Carrington, C. V., 2012. Phylogeography and population dynamics of dengue viruses in the americas. Mol. Biol. Evol. 29 (6), 1533–1543.

Araujo, J. M., Nogueira, R. M., Schatzmayr, H. G., Zanotto, P. M., Bello, G., 2009. Phylogeography and evolutionary history of dengue virus type 3. Infect. Genet. Evol. 9, 716–725.

Baele, G., Lemey, P., Bedford, T., Rambaut, A., Suchard, M. A., Alekseyenko, A. V., 2012. Improving the Accuracy of Demographic and Molecular Clock Model Comparison While Accommodating Phylogenetic Uncertainty. Mol Biol Evol.

Bahl, J., Nelson, M. I., Chan, K. H., Chen, R., Vijaykrishna, D., Halpin, R. A., Stockwell, T. B., Lin, X., Wentworth, D. E., Ghedin, E., Guan, Y., Peiris, J. S., Riley, S., Rambaut, A., Holmes, E. C., Smith, G. J., 2011. Temporally structured metapopulation dynamics and persistence of influenza A H3N2 virus in humans. Proc. Natl. Acad. Sci. U.S.A. 108 (48), 19359–19364.

Balinda, S. N., Sangula, A. K., Heller, R., Muwanika, V. B., Belsham, G. J., Masembe, C., Siegismund, H. R., 2010. Diversity and transboundary mobility of serotype O foot-and-mouth disease virus in East Africa: implications for vaccination policies. Infect. Genet. Evol. 10, 1058–1065.

Biek, R., Henderson, J. C., Waller, L. A., Rupprecht, C. E., Real, L. A., 2007. A high-resolution genetic signature of demographic and spatial expansion in epizootic rabies virus. Proc. Natl. Acad. Sci. U.S.A. 104, 7993–7998.

Biek, R., Real, L. A., 2010. The landscape genetics of infectious disease emergence and spread. Mol. Ecol. 19, 3515–3531.

Bielejec, F., Rambaut, A., Suchard, M. A., Lemey, P., 2011. SPREAD: spatial phylogenetic reconstruction of evolutionary dynamics. Bioinformatics 27, 2910–2912.

Carvalho, L., Santos, L., Pereira, P., Silveira, W., 2011. Phylodynamics of foot-and-mouth disease virus: a complex network approach. In: Proceedings of the 10th Brazilian Conference on Dynamics, Control and Their Applications. Brazilian Society for Applied and Computational Mathematics.

Cottam, E. M., Thebaud, G., Wadsworth, J., Gloster, J., Mansley, L., Paton, D. J., King, D. P., Haydon, D. T., 2008. Integrating genetic and epidemiological data to determine transmission pathways of foot-and-mouth disease virus. Proc. Biol. Sci. 275, 887–895.

Drummond, A. J., Ho, S. Y., Phillips, M. J., Rambaut, A., 2006. Relaxed phylogenetics and dating with confidence. PLoS Biol. 4, e88.

Drummond, A. J., Rambaut, A., 2007. BEAST: Bayesian evolutionary analysis by sampling trees. BMC Evol. Biol. 7, 214.

Drummond, A. J., Rambaut, A., Shapiro, B., Pybus, O. G., 2005. Bayesian coalescent inference of past population dynamics from molecular sequences. Mol. Biol. Evol. 22, 1185–1192.

Etherington, G. J., Dicks, J., Roberts, I. N., 2005. Recombination Analysis Tool (RAT): a program for the high-throughput detection of recombination. Bioinformatics 21, 278–281.

Faria, N. R., Suchard, M. A., Abecasis, A., Sousa, J. D., Ndembi, N., Bonfim, I., Camacho, R. J., Vandamme, A. M., Lemey, P., 2012. Phylodynamics of the HIV-1 CRF02_AG clade in Cameroon. Infect. Genet. Evol. 12 (2), 453–460.

Faria, N. R., Suchard, M. A., Rambaut, A., Lemey, P., 2011. Toward a quantitative understanding of viral phylogeography. Curr Opin Virol 1 (5), 423–429.

Ferreira, M. A. R., Suchard, M. A., 2008. Bayesian Analysis of elapsed times in continuous-time Markov chains. Canadian Journal of Statistics. 26, 355–368.

14

Green, D. M., Kiss, I. Z., Kao, R. R., 2006. Modelling the initial spread of foot-and-mouth disease through animal movements. Proc. Biol. Sci. 273, 2729–2735.

Guillot, G., Leblois, R., Coulon, A., Frantz, A. C., 2009. Statistical methods in spatial genetics. Mol. Ecol. 18, 4734–4756.

Hasegawa, M., Kishino, H., Yano, T., 1985. Dating of the human-ape splitting by a molecular clock of mitochondrial DNA. J. Mol. Evol. 22, 160–174.

Kuhnert, D., Wu, C. H., Drummond, A. J., 2011. Phylogenetic and epidemic modeling of rapidly evolving infectious diseases. Infect. Genet. Evol. 11 (8), 1825–1841.

Lemey, P., Rambaut, A., Drummond, A. J., Suchard, M. A., 2009. Bayesian phylogeography finds its roots. PLoS Comput. Biol. 5, e1000520.

Lindholm, A., Hewitt, E., Torres, P., Medardo, L., Escheverria, C.and Shaw, J., Hernandez, J., 2007. Epidemiologic aspects of a foot-and-mouth disease epidemic in cattle in ecuador. J. Appl. Res. Vet. Med. 5, 17–24.

Malirat, V., Bergmann, I. E., Campos, R. d. e. M., Salgado, G., Sanchez, C., Conde, F., Quiroga, J. L., Ortiz, S., 2011. Phylogenetic analysis of Foot-and-Mouth Disease Virus type O circulating in the Andean region of South America during 2002-2008. Vet. Microbiol. 152, 74–87.

Malirat, V., de Barros, J. J., Bergmann, I. E., Campos, R. d. e. M., Neitzert, E., da Costa, E. V., da Silva, E. E., Falczuk, A. J., Pinheiro, D. S., de Vergara, N., Cirvera, J. L., Maradei, E., Di Landro, R., 2007. Phylogenetic analysis of foot-and-mouth disease virus type O re-emerging in free areas of South America. Virus Res. 124, 22–28.

Maradei, E., Perez Beascoechea, C., Malirat, V., Salgado, G., Seki, C., Pedemonte, A., Bonastre, P., D'Aloia, R., La Torre, J. L., Mattion, N., Rodriguez Toledo, J., Bergmann, I. E., 2011. Characterization of foot-and-mouth disease virus from outbreaks in Ecuador during 2009-2010 and cross-protection studies with the vaccine strain in use in the region. Vaccine 29, 8230–8240.

Mondini, A., de Moraes Bronzoni, R. V., Nunes, S. H., Chiaravalloti Neto, F., Massad, E., Alonso, W. J., Lazzaro, E. S., Ferraz, A. A., de Andrade Zanotto, P. M., Nogueira, M. L., 2009. Spatio-temporal tracking and phylodynamics of an urban dengue 3 outbreak in So Paulo, Brazil. PLoS Negl Trop Dis 3, e448.

Nelson, M. I., Lemey, P., Tan, Y., Vincent, A., Lam, T. T., Detmer, S., Viboud, C., Suchard, M. A., Rambaut, A., Holmes, E. C., Gramer, M., 2011. Spatial dynamics of human-origin H1 influenza A virus in North American swine. PLoS Pathog. 7 (6), e1002077.

Openshaw, S., 1984. Ecological fallacies and the analysis of areal census data. Environ. Plan. A 16, 17–31.

PAHO/WHO, 2006. Situación de los Programas de Erradicación de la Fiebre Aftosa en America del Sur, 2005. Pan American Center for Foot-and-Mouth Disease 1, 40.

PAHO/WHO, 2008. Situación de los Programas de Erradicación de la Fiebre Aftosa en America del Sur, 2007. Pan American Center for Foot-and-Mouth Disease 1, 67.

Parker, J., Rambaut, A., Pybus, O. G., 2008. Correlating viral phenotypes with phylogeny: accounting for phylogenetic uncertainty. Infect. Genet. Evol. 8 (3), 239–246.

Ploegh, H. L., 1998. Viral strategies of immune evasion. Science 280, 248–253.

Posada, D., 2008. jModelTest: phylogenetic model averaging. Mol. Biol. Evol. 25, 1253–1256.

Rabaa, M. A., Ty Hang, V. T., Wills, B., Farrar, J., Simmons, C. P., Holmes, E. C., 2010. Phylogeography of recently emerged DENV-2 in southern Viet Nam. PLoS Negl Trop Dis 4 (7), e766.

Samuel, A. R., Knowles, N. J., 2001. Foot-and-mouth disease type O viruses exhibit genetically and geographically distinct evolutionary lineages (topotypes). J. Gen. Virol. 82, 609–621.

Sangula, A. K., Belsham, G. J., Muwanika, V. B., Heller, R., Balinda, S. N., Masembe, C., Siegismund, H. R., 2010. Evolutionary analysis of foot-and-mouth disease virus serotype SAT 1 isolates from east Africa suggests two independent introductions from southern Africa. BMC Evol. Biol. 10, 371.

Shim, E., Galvani, A. P., 2009. Evolutionary repercussions of avian culling on host resistance and influenza virulence. PLoS ONE 4 (5), e5503.

Tamura, K., Peterson, D., Peterson, N., Stecher, G., Nei, M., Kumar, S., 2011. MEGA5: molecular evolutionary genetics analysis using maximum likelihood, evolutionary distance, and maximum parsimony methods. Mol. Biol. Evol. 28, 2731–2739.

Yoon, S. H., Park, W., King, D. P., Kim, H., 2011. Phylogenomics and molecular evolution of foot-and-mouth disease virus. Mol. Cells 31, 413–421.
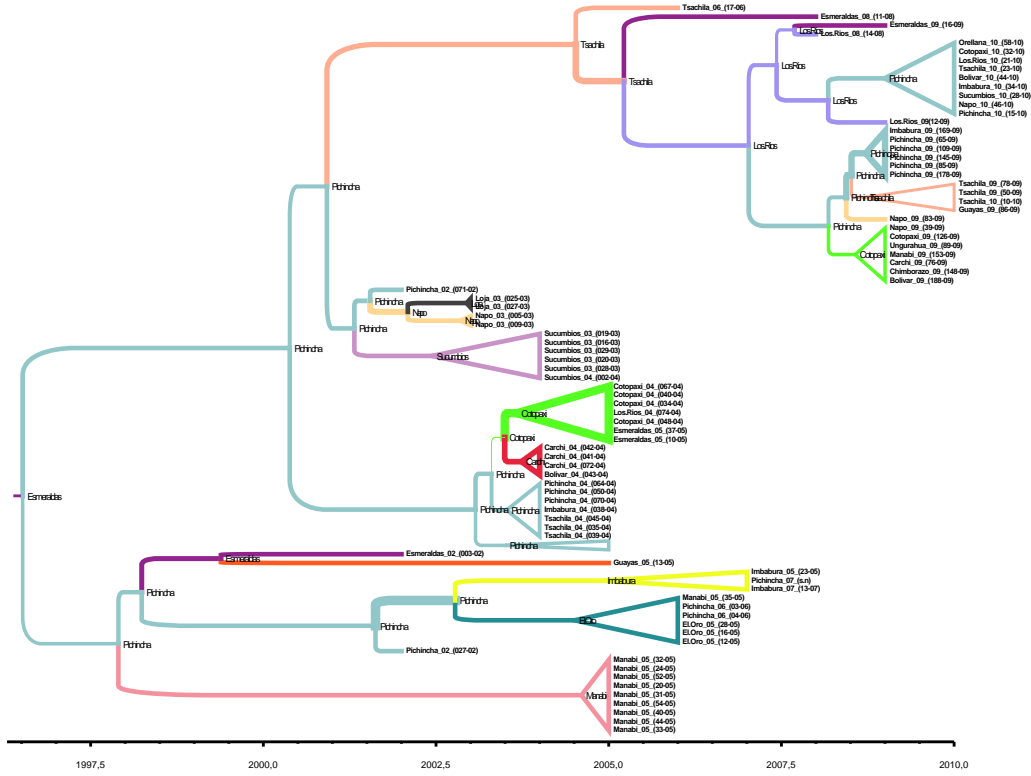
Figure 1: Midpoint rooted, time-structured maximum clade credibility (MCC) tree obtained for the province-level dataset. Some terminal nodes were collapsed for clarity. Thickness of branches is proportional to rates of evolution and colors depict the most probable origin of the branch. Internal nodes' labels show the most probable province of origin of each node of the tree.
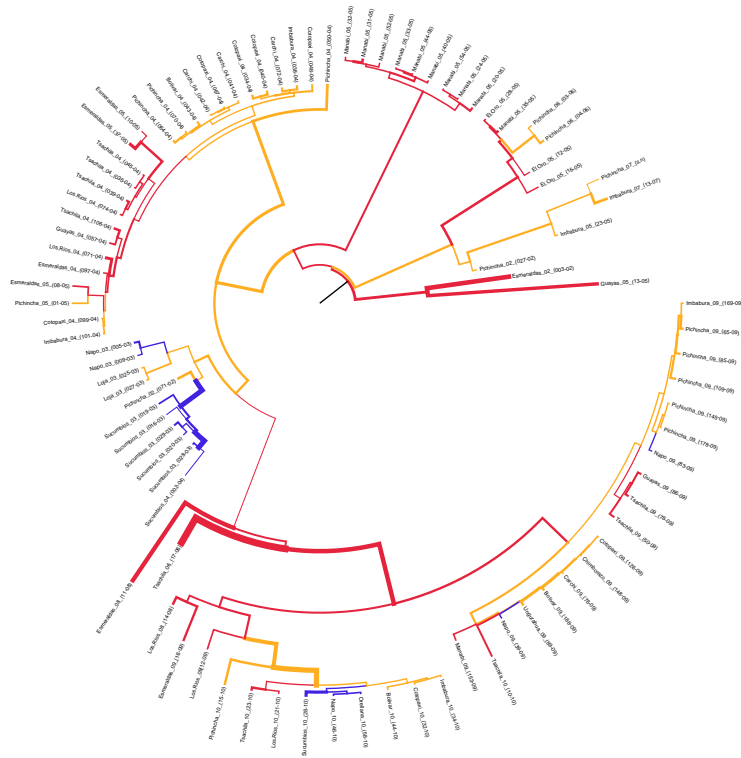
Figure 2: Unrooted maximum clade credibility (MCC) tree obtained with the data aggregated to the region level. Thickness of branches is proportional to rates of evolution and colors depict the ecologic regions of Ecuador. Yellow–Highland, red–Coast,blue–Amazon.
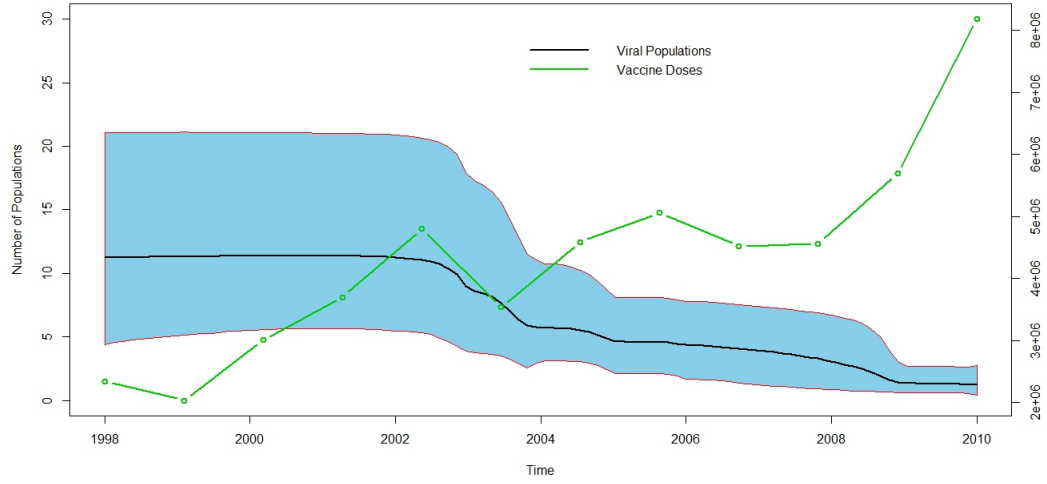
Figure 3: Bayesian skyline representing the past population of FMDV in Ecuador, solid line stands for the median and blue envelopes represent 95 % Bayesian credible intervals. We also show the number of vaccine doses applied per year in Ecuador (green dotted line).

20
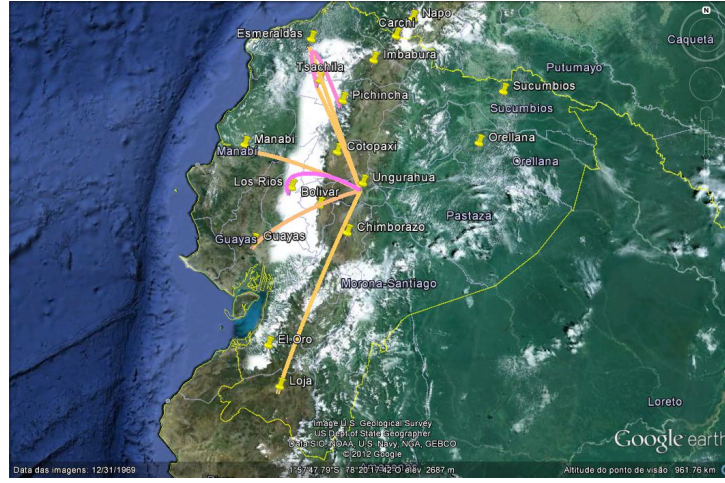
(a)
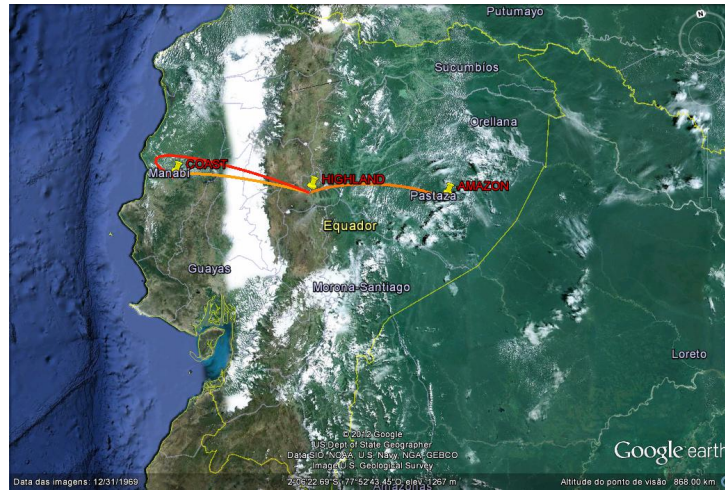
(b)

Figure 4: Bayes factors analysis from Bayesian Stochastic Search Variable Selection. We present the most significant routes (colored lines) of spread for FMDV in Ecuador, obtained by applying a cutoff of 6 to Bayes Factors from BSSVS for province-level data (a) and a cutoff of 30 to (b) region-level data. Lighter tones indicate larger BFs and the tack marks indicate the centroids for each province/region.
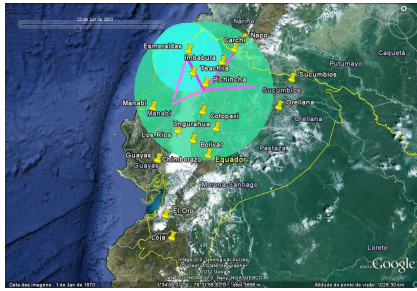
(a) 2002
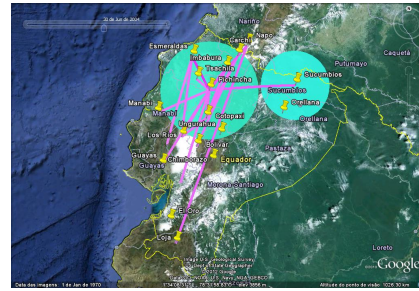
(b) 2004
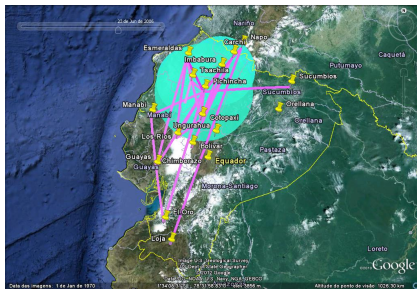
(c) 2006
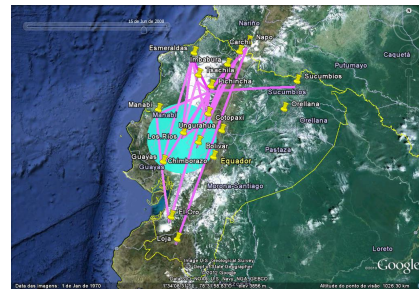
(d) 2008
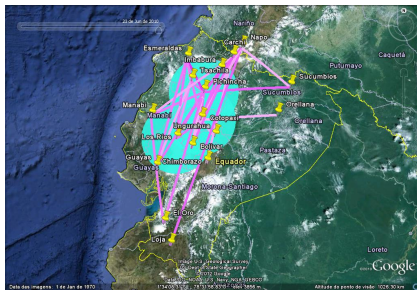
(e) 2010

Figure 5: Inferred routes of spread of FMDV in Ecuador for the years of 2002, 2004, 2008 and 2010. Spatio-temporal dynamics of FMDV in Ecuador is marked by a densely connected network of migration routes (colored lines), suggesting an intense flow of infected animals throughout the country. The radius of the circles are proportional to the number of lineages, lighter tones indicate more recent times of transition and tack marks indicate the centroids for each province. The images were generated with the SPREAD (Bielejec et al., 2011) software and visualized with Google Earth.

22

Evolutionary Parameter	Mean (BCI)
Clock rate (subst/site/year X 10^{-2})	1.10 (0.73–1.42)
Clock rate coefficient of variation	1.02 (0.90–1.14)
1st Codon[a]	0.59 (0.51–0.61)
2nd Codon	0.60 (0.53–0.61)
3rd Codon	1.87 (1.62–1.91)
TMRCA[b] (years)	13.7 (10.7–17.5)

Table 1: Summary statistics of the evolutionary analyses presented in this study. We report the Bayesian estimates for evolutionary parameters and their 95 % Bayesian credible intervals. a–relative contribution of each codon position; b–Time to Most Recent Common Ancestor.

ρ	λ	Log-likelihood	AICM (SE)	$\mathbf{W}$ (BCI)
0.00	$log(2)$	-4034.74	7676.34 (0.43)	18 (16-20)
0.00	16	-4024.57	7650.01 (0.39)	35 (28-42)
0.05	**22**	**-4024.51**	**7646.01 (0.56)**	**40 (32-49)**
0.10	**28**	**-4024.49**	**7646.07 (0.38)**	**46 (37-56)**
0.20	40	-4026.42	7647.25 (0.59)	57 (46-69)
0.30	52	-4022.71	7654.86 (0.52)	68 (55-82)

Table 2: Comparison of different scenarios of viral flow intensity (see Appendix for details). We report the median and 95% Bayesian Credible Intervals (BCI) for the number of non-zero rates ($\mathbf{W}$) obtained for each model. Each intensity model was evaluated by log marginal likelihood calculated using path sampling and AICM with Monte Carlo standard errors (SE) calculated using 1000 replicates. The best models are highlighted in boldface.

Model	Log-likelihood	AICM (SE)	lnBF
Distance Informed	-3982.8	7538.92 (0.76)	5.1
Herd size	**-3981.3**	**7532.96 (1.63)**	**6.6**
Herd density	-3984.5	7544.92 (0.86)	3.4
Vaccination Coverage	-3985.3	7542.26 (0.32)	2.6
Non-Informative	-3987.9	7552.94 (0.31)	-

Table 3: Incorporation of host population variables. Different prior distributions were parameterized for the rates of transition in the CTMC model, and comparison between different predictors was made by log-likelihood and AICM. Marginal likelihoods were calculated through path sampling and AICM's Monte Carlo standard errors (SE) were calculated using 1000 bootstrap replicates. We report log Bayes Factors (natural base) to the non-informative prior model and highlight the best model in bold face.

Province	$Pr(root)$	Region	$Pr(root)$
Bolívar	0.021	Amazon region	0.009
Carchi	0.015	**Coast region**	**0.624**
Chimborazo	0.007	Highland region	0.365
Cotopaxi	0.069		
El Oro	0.050		
Esmeraldas	**0.193**		
Guayas	0.073		
Imbabura	0.080		
Loja	0.087		
Los Rios	0.070		
Manabi	0.039		
Napo	0.040		
Orellana	0.009		
Pichincha	0.180		
S. D. de los Tsachilas	0.010		
Sucumbios	0.020		
Tungurahaua	0.007		

Table 4: Analysis of the spatial origins of FMDV in Ecuador. The probability of being the origin of the circulating strains, $Pr(root)$, is reported for all provinces and regions and the highest values for each aggregation scheme are highlighted in bold face.

6. Appendix

6.1. Prior specification

As we use Bayesian Stochastic Search Variable Selection (BSSVS) (Lemey et al., 2009) to search a set of significant rates of viral dispersal required to explain the dispersal process, each entry of the CTMC's transition matrix is transformed into a binary indicator variable. We assume that these indicator variables are independent realizations of a Bernoulli process with small success probability, which sum is the number of non-zero rates, $\mathbf{W}$ (Lemey et al., 2009). Biologically, this quantity reflects the overall intensity of the flow of viral strains between regions. To parameterize prior distributions on $\mathbf{W}$ and simulate several intensity scenarios we assume that the transition matrix is symmetric and that the minimum number of routes, $K-1$, is supplemented with a proportion ρ of the remaining off-diagonal entries and follows a truncated poisson (TP) distribution such that:

$$\mathbf{W} \sim \mathrm{TP}(\lambda = K - 1 + \rho[(K^2 - 3K + 2)/2], \mathrm{offset} = K - 1) \qquad (1)$$

By choosing any $\rho \in [0,1]$, one can simulate various intensity scenarios. Here we choose $\rho =0.05$, 0.10, 0.20 and 0.30.

To complete the specification of the model we propose a prior distribution on the infinitesimal rate matrix, $\mathbf{S}$, incorporating various epidemiologically relevant variables. For instance, to formulate a distance-informed prior we assume a multivariate gamma distribution with expectations m_{jk} and unit coefficient of variation according to:

$$m_{jk} = C \frac{d_{jk}^{-1}}{\sum_{j<k} d_{jk}^{-1}}, \mathbf{S} \sim MG_{K-1}(\mathbf{1}, m_{jk}) \qquad (2)$$

where $\mathbf{1}$ is a unit vector which dimension equals the degree of $\mathbf{S}$, d_{jk} is the great-circle distance between the centroids of regions k and j and C is an arbitrary normalization constant (Lemey et al., 2009). Note that this formulation follows from the hypothesis that more distant regions have lower migration rates between them.

In order to incorporate other epidemiologically relevant variables into the analysis we follow a similar approach to that above and formulate the priors on $\mathbf{S}$ by assuming a gravity model (Nelson et al., 2011). For instance, we can parameterize a population-based gravity model assuming that rate of viral

25

flow is proportional to the difference between herd sizes of two regions:

$$m^p_{jk} = C \frac{|p_j - p_k|}{\sum_{j<k} |p_j - p_k|} \tag{3}$$

Likewise, gravity priors for herd density (m^d_{jk}) and vaccination (m^v_{jk}) were formulated assuming that viral flow between two locations is directly proportional to the difference their population densities and vaccination coverage.

GenBank ID	COUNTRY	PROVINCE	LAT	LON	YEAR	GenBank ID	COUNTRY	PROVINCE	LAT	LON	YEAR
JN005918.1	Ecuador	Orellana	-0.73	-76.9	2010	HQ695843.1	Ecuador	Los Rios	-1.34	-79.49	2004
JN005916.1	Ecuador	Napo	0.99	-77.82	2010	HQ695841.1	Ecuador	Carchi	0.74	-78.05	2004
JN005914.1	Ecuador	Bolivar	-1.59	-79.1	2010	HQ695839.1	Ecuador	Los Rios	-1.34	-79.49	2004
JN005912.1	Ecuador	Imbabura	0.41	-78.36	2010	HQ695837.1	Ecuador	Pichincha	-0.15	-78.78	2004
JN005910.1	Ecuador	Cotopaxi	-0.86	-78.86	2010	HQ695835.1	Ecuador	Cotopaxi	-0.86	-78.86	2004
JN005908.1	Ecuador	Sucumbios	-0.02	-76.56	2010	HQ695833.1	Ecuador	Pichincha	-0.15	-78.78	2004
JN005906.1	Ecuador	Tsachila	0.14	-79.1	2010	HQ695831.1	Ecuador	Guayas	-2.09	-80.01	2004
JN005904.1	Ecuador	Los Rios	-1.34	-79.49	2010	HQ695829.1	Ecuador	Pichincha	-0.15	-78.78	2004
JN005902.1	Ecuador	Pichincha	-0.15	-78.78	2010	HQ695827.1	Ecuador	Cotopaxi	-0.86	-78.86	2004
JN005900.1	Ecuador	Tsachila	0.14	-79.1	2010	HQ695825.1	Ecuador	Tsachila	0.14	-79.1	2004
JN005898.1	Ecuador	Bolivar	-1.59	-79.1	2009	HQ695823.1	Ecuador	Bolivar	-1.59	-79.1	2004
JN005896.1	Ecuador	Pichincha	-0.15	-78.78	2009	HQ695821.1	Ecuador	Carchi	0.74	-78.05	2004
JN005894.1	Ecuador	Imbabura	0.41	-78.36	2009	HQ695819.1	Ecuador	Carchi	0.74	-78.05	2004
JN005892.1	Ecuador	Manabi	-0.75	-80.13	2009	HQ695817.1	Ecuador	Cotopaxi	-0.86	-78.86	2004
JN005890.1	Ecuador	Chimborazo	-1.97	-78.72	2009	HQ695815.1	Ecuador	Tsachila	0.14	-79.1	2004
JN005917.1	Ecuador	Pichincha	-0.15	-78.78	2009	HQ695813.1	Ecuador	Imbabura	0.41	-78.36	2004
JN005915.1	Ecuador	Cotopaxi	-0.86	-78.86	2009	HQ695811.1	Ecuador	Tsachila	0.14	-79.1	2004
JN005913.1	Ecuador	Pichincha	-0.15	-78.78	2009	HQ695809.1	Ecuador	Cotopaxi	-0.86	-78.86	2004
JN005911.1	Ecuador	Tungurahua	-1.29	-78.5	2009	HQ695807.1	Ecuador	Sucumbios	-0.02	-76.56	2004
JN005909.1	Ecuador	Guayas	-2.09	-80.01	2009	HQ695805.1	Ecuador	Sucumbios	-0.02	-76.56	2003
JN005907.1	Ecuador	Pichincha	-0.15	-78.78	2009	HQ695803.1	Ecuador	Sucumbios	-0.02	-76.56	2003
JN005905.1	Ecuador	Napo	0.99	-77.82	2009	HQ695801.1	Ecuador	Loja	-4.09	-79.65	2003
JN005903.1	Ecuador	Tsachila	0.14	-79.1	2009	HQ695799.1	Ecuador	Loja	-4.09	-79.65	2003
JN005901.1	Ecuador	Carchi	0.74	-78.05	2009	HQ695797.1	Ecuador	Sucumbios	-0.02	-76.56	2003
JN005899.1	Ecuador	Pichincha	-0.15	-78.78	2009	HQ695795.1	Ecuador	Sucumbios	-0.02	-76.56	2003
JN005897.1	Ecuador	Tsachila	0.14	-79.1	2009	HQ695793.1	Ecuador	Sucumbios	-0.02	-76.56	2003
JN005895.1	Ecuador	Napo	0.99	-77.82	2009	HQ695791.1	Ecuador	Napo	0.99	-77.82	2003
JN005893.1	Ecuador	Esmeraldas	0.71	-79.22	2009	HQ695789.1	Ecuador	Napo	0.99	-77.82	2003
JN005891.1	Ecuador	Los Rios	-1.34	-79.49	2009	HQ695787.1	Ecuador	Pichincha	-0.15	-78.78	2002
HQ695842.1	Ecuador	Los Rios	-1.34	-79.49	2008	HQ695785.1	Ecuador	Pichincha	-0.15	-78.78	2002
HQ695840.1	Ecuador	Esmeraldas	0.71	-79.22	2008	HQ695783.1	Ecuador	Esmeraldas	0.71	-79.22	2002
HQ695838.1	Ecuador	Pichincha	-0.15	-78.78	2007	HQ695844.1	Peru	Lima	-	-	1994
HQ695836.1	Ecuador	Imbabura	0.41	-78.36	2007	HQ695770.1	Colombia	Narino	-	-	1998
HQ695834.1	Ecuador	Tsachila	0.14	-79.1	2006	HQ695771.1	Colombia	Cauca	-	-	1998
HQ695832.1	Ecuador	Pichincha	-0.15	-78.78	2006	HQ695763.1	Colombia	Cundinamarca	-	-	1995
HQ695830.1	Ecuador	Pichincha	-0.15	-78.78	2006	HQ695778.1	Colombia	Narino	-	-	2000
HQ695828.1	Ecuador	Manabi	-0.75	-80.13	2005	HQ695758.1	Colombia	Cauca	-	-	1994
HQ695826.1	Ecuador	Manabi	-0.75	-80.13	2005	HQ695762.1	Colombia	Casanare	-	-	1994
HQ695824.1	Ecuador	Manabi	-0.75	-80.13	2005	HQ695845.1	Venezuela	Yaracuy	-	-	2003
HQ695822.1	Ecuador	Manabi	-0.75	-80.13	2005	HQ695781.1	Colombia	Santander	-	-	2008
HQ695820.1	Ecuador	Esmeraldas	0.71	-79.22	2005	HQ695847.1	Venezuela	Trujillo	-	-	2005
HQ695818.1	Ecuador	Manabi	-0.75	-80.13	2005	HQ695849.1	Venezuela	Trujillo	-	-	2006
HQ695816.1	Ecuador	Manabi	-0.75	-80.13	2005	HQ695750.1	Colombia	Boyaca	-	-	1994
HQ695814.1	Ecuador	Manabi	-0.75	-80.13	2005	HQ695752.1	Colombia	Valle	-	-	1994
HQ695812.1	Ecuador	Manabi	-0.75	-80.13	2005	HQ695749.1	Colombia	Boyaca	-	-	1994
HQ695810.1	Ecuador	El Oro	-3.52	-79.81	2005	HQ695754.1	Colombia	Cundinamarca	-	-	1994
HQ695808.1	Ecuador	Manabi	-0.75	-80.13	2005	HQ695756.1	Colombia	Cundinamarca	-	-	1994
HQ695806.1	Ecuador	Imbabura	0.41	-78.36	2005	HQ695743.1	Bolivia	La Paz	-	-	2002
HQ695804.1	Ecuador	Manabi	-0.75	-80.13	2005	HQ695741.1	Bolivia	Beni	-	-	2001
HQ695802.1	Ecuador	El Oro	-3.52	-79.81	2005	HQ695739.1	Bolivia	Potosi	-	-	2001
HQ695800.1	Ecuador	Guayas	-2.09	-80.01	2005	DQ834709.1	Bolivia	Tarija	-	-	2001
HQ695798.1	Ecuador	El Oro	-3.52	-79.81	2005	DQ834706.1	Brazil	RS	-	-	2000
HQ695796.1	Ecuador	Esmeraldas	0.71	-79.22	2005	DQ834711.1	Paraguay	PozoHondo	-	-	2003
HQ695794.1	Ecuador	Esmeraldas	0.71	-79.22	2005	DQ834727.1	Argentina	Corrientes	-	-	2006
HQ695792.1	Ecuador	Pichincha	-0.15	-78.78	2005	DQ834714.1	Brazil	MS	-	-	2005
HQ695790.1	Ecuador	Tsachila	0.14	-79.1	2004	DQ834715.1	Brazil	MS	-	-	2005
HQ695788.1	Ecuador	Imbabura	0.41	-78.36	2004	DQ834707.1	Uruguay	Artigas	-	-	2000
HQ695786.1	Ecuador	Cotopaxi	-0.86	-78.86	2004	DQ834710.1	Paraguay	Canindeyu	-	-	2002
HQ695784.1	Ecuador	Esmeraldas	0.71	-79.22	2004	DQ834705.1	Argentina	-	-	-	2000

Table 5: A.Table 1. Acession Numbers (GenBank IDs) and spatio-temporal information about the sequences used in this study.

Province	Herd Size (heads)	Area (Km^2)	Herd density (heads/Km^2)
Bolivar	196523	380812	0.52
Carchi	93784	174209	0.54
Cotopaxi	193129	457199	0.42
Chimborazo	246787	471444	0.52
Imbabura	105057	283659	0.37
Loja	361455	994854	0.36
Pichincha	444573	925740	0.48
Tungurahua	151258	204083	0.74
El Oro	162467	457025	0.36
Esmeraldas	219385	785842	0.28
Guayas	344798	1315023	0.26
Los Rios	117803	637307	0.18
Manabi	783592	1583661	0.49
Morona Santiago	229205	891435	0.26
Napo	50984	288424	0.18
Sucumbios	49591	356481	0.14
Orellana	35942	250172	0.14
Moran's I (p-value)^a	0.30 (< 0.01)	0.15 (0.13)	0.31 (< 0.01)

Table 6: A.Table 2. Cattle population data used in this study.a–Moran's I index statistic and the associated p-value were computed for each variable using 10,000 Markov chain Monte Carlo permutations.

Province	2006	2007	2008	2009	2010	Mean[a]
Bolivar	11	15	24	71	70	38.2
Carchi	62	68	87	100	100	83.4
Cotopaxi	34	32	51	88	100	61.0
Chimborazo	14	12	18	62	63	33.8
Imbabura	33	36	53	77	85	56.8
Loja	12	11	20	39	41	24.6
Pichincha	100	100	100	100	100	100.0
Tungurahua	16	13	28	63	64	36.8
El Oro	58	65	88	100	100	82.2
Esmeraldas	93	85	100	100	100	95.6
Guayas	77	95	100	100	100	94.4
Los Rios	63	52	57	78	95	69.0
Manabi	66	64	85	100	100	83.0
Morona Santiago	41	35	45	59	60	48.0
Napo	55	73	74	97	100	79.8
Sucumbios	37	72	100	100	100	81.8
Orellana	68	97	100	100	100	93.0
Moran's I (p-value)[b]	0.19 (0.04)	0.21 (0.03)	0.17 (0.06)	0.25 (0.01)	0.21 (0.04)	0.35 (< 0.01)

Table 7: A.Table 3. Vaccination data used in this study (%). a-Annual mean calculated as arithmetic mean of vaccination coverage for the period (2006-2010), b–Moran's I index statistic and the associated p-value were computed for each variable using 10,000 Markov chain Monte Carlo permutations.

Coalescent	Clock model	Log-Likelihood	AICM (SE)
Constant	ULN	-3586.9	6820.33 (0.54)
Expansion Growth	ULN	-3581.9	6810.36 (0.24)
Exponential Growth	ULN	-3587.0	6810.91 (0.15)
Skyline	ULN	-3569.4	6808.63 (0.45)
Constant	UCE	-3574.4	6792.95 (0.39)
Expansion Growth	UCE	-3573.9	6798.46 (0.33)
Exponential Growth	UCE	-3585.2	6799.25 (0.32)
Skyline	UCE	**-3561.6**	**6778.26 (0.48)**

Table 8: A.Table 4. Results from the initial optmization study. Several coalescent priors and clock models were compared by log marginal likelihood and AICM, the best model highlighted in boldface. We used path sampling to obtain the log-likelihoods and 1000 bootstrap replicates to estimate the standard errors (SE) for AICM. All comparisons are based on equal amounts of independent Monte Carlo samples. ULN=uncorrelated log-normal; UCE= uncorrelated exponential.
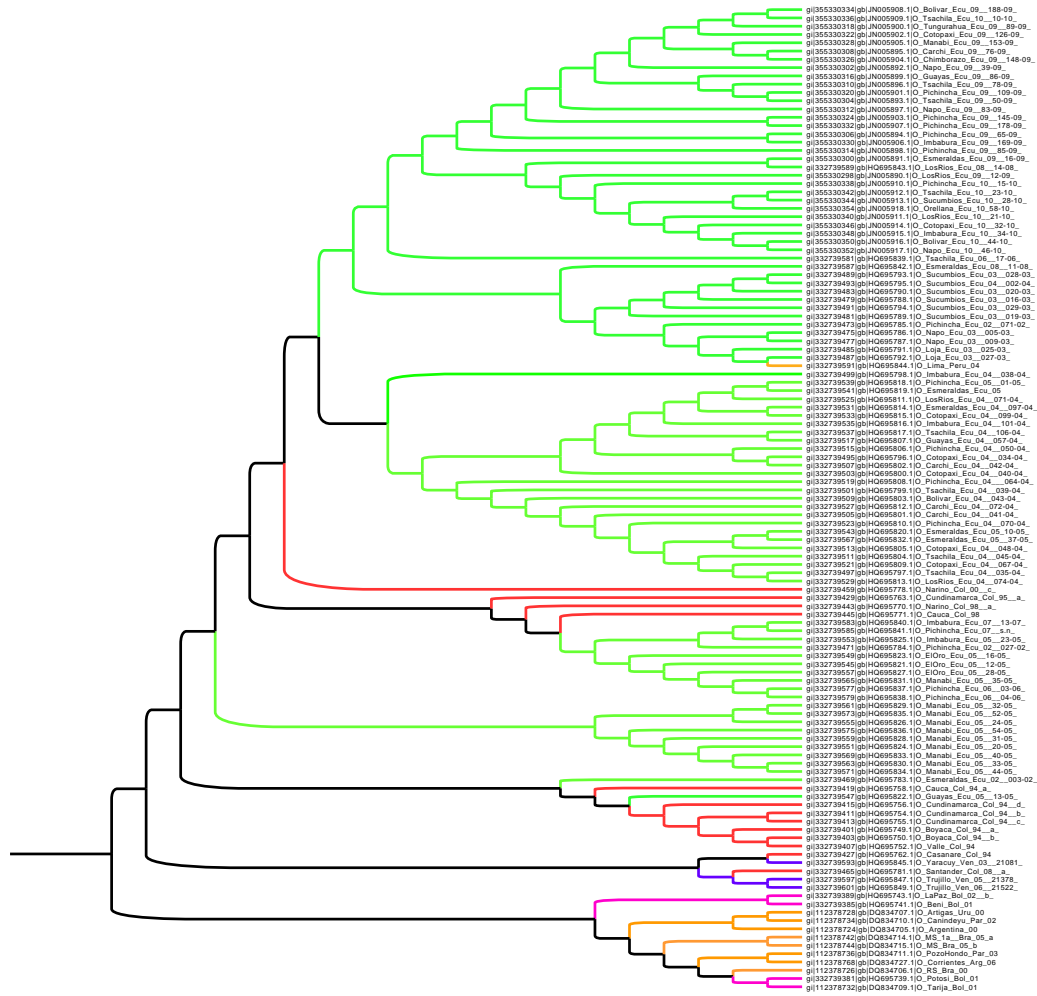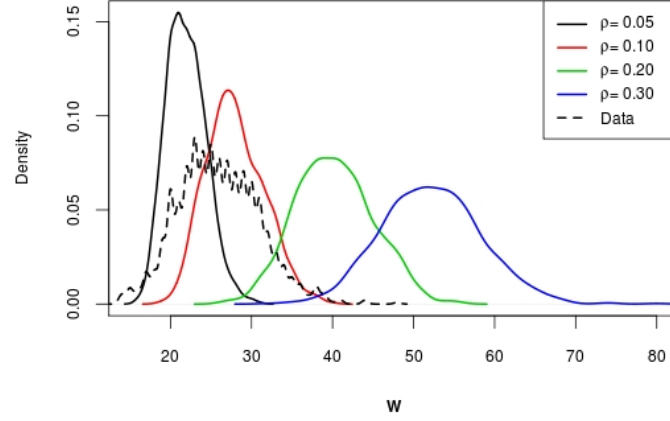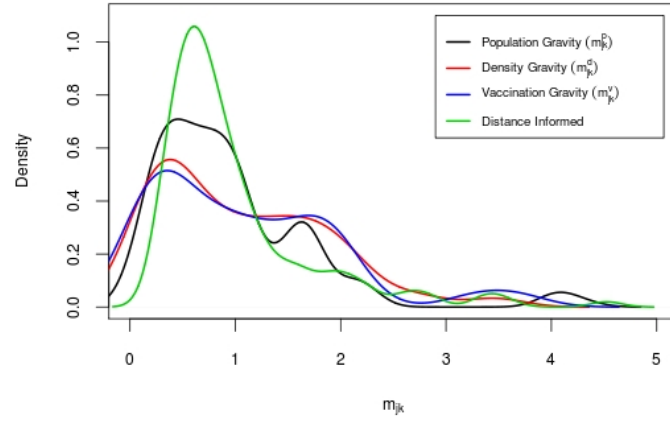
Figure 6: A1. Maximum Likelihood (ML) cladogram depicting South American FMDV serotype O isolates. It is shown that Ecuadorian isolates tend to cluster together despite being interleaved with sequences from Colombia. Legend: Ecuador-green; Colombia-red; Venezuela-blue; Bolivia-pink; Souther Cone (Brazil, Argentina, Uruguay and Paraguay)-orange.

31

(a)

(b)

Figure 7: A2. Plot of the prior distributions used in this study. In (a) we illustrate the various intensity scenarios on **W** along with the distribution of non-zero rates in the spatial transition matrix yielded by the best model ("Data") and in (b) models for the infinitesimal rate matrix **S** based on epidemiologically relevant variables are shown (see Methods, section 2.3.1 for details)
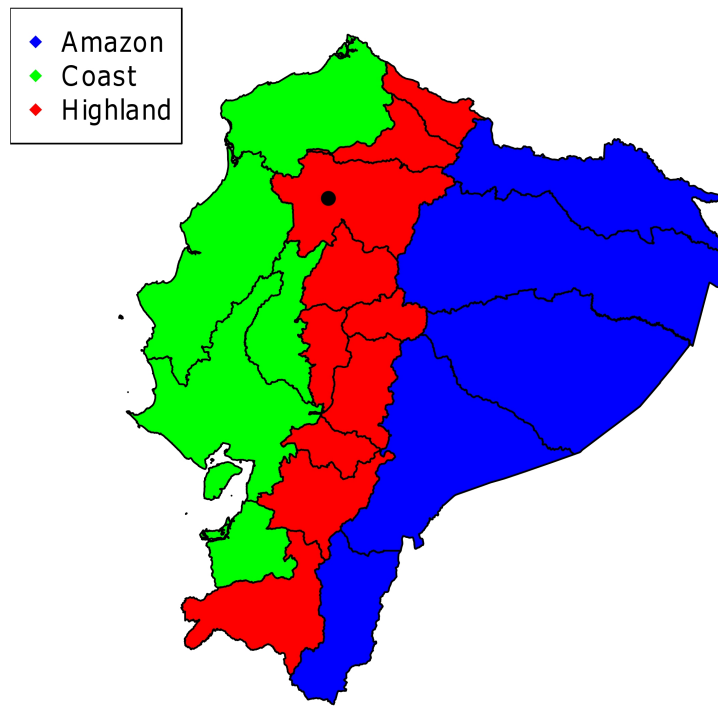
Figure 8: A3. Map of Ecuador showing its three main ecological regions. The solid black circle marks the localization of the Santo Domingo's animal fair.